Macroporous Silicon

Noureddine Gabouze and François Ozanam

Contents

Abstract

The electrochemical formation of macropores in porous silicon is briefly reviewed. Various morphologies are obtained as a function of the substrate type and etching conditions. On n-Si, macropores are generally growing along preferential crystallographic directions. On p-Si, in aqueous conditions far from electropolishing, the growth direction is rather determined by the current lines in the space-charge region. A summary of macropore characteristics is given as a function of the preparation conditions. Various models have been developed in order to account for the morphologies and characteristic sizes. These joint experimental and theoretical works have provided a good

N. Gabouze (✉)
Centre de Recherche sur la Technologie des Semi-conducteurs et l'Energie (CRTSE), Algiers, Algeria
e-mail: gabouzenoureddine@crtse.dz

F. Ozanam
Physique de la Matière Condensée, CNRS-Ecole polytechnique, Palaiseau, France
e-mail: francois.ozanam@polytechnique.edu

© Springer International Publishing AG, part of Springer Nature 2018

L. Canham (ed.), *Handbook of Porous Silicon*,
https://doi.org/10.1007/978-3-319-71381-6_10

understanding of macropore growth, opening the way to many applications, and the most significant ones are mentioned. An impressive level of control has eventually been achieved for the fabrication of regular macropore arrays of high aspect ratio, including the incorporation of intentional defects or pore-wall shaping.

Keywords
Crystallography · Electrolyte resistivity · Lehmann's model · Macropore formation · Macroporous silicon

Introduction

According to the IUPAC standard, macropores correspond to pores exhibiting characteristic sizes (pore diameter and average distance between pores) larger than 50 nm. The term "macropore" is usually associated with smooth cylindrical pores with characteristic sizes on the order of 1 μm.

This kind of pore can be obtained under a variety of conditions and with differing morphologies (see chapter ▶ "Routes of Formation for Porous Silicon"). In this review, we focus on electrochemically etched macropores. The key parameters are the electrolyte type [aqueous (aqu), organic (org), oxidant (ox)] the HF concentration, the surfactant, the Si doping type and level (n, n^+, p, p^+), and in some cases the illumination [backside illumination (bsi) or frontside illumination (fsi)]. Detailed reviews regarding their formation are available (Föll et al. 2002; Lehmann 2005; Chazalviel and Ozanam 2005; Lehmann 2002; and handbook chapter ▶ "Porous Silicon Formation by Anodization").

Current-Line- and Crystallography-Driven Macropores

Two distinct classes of macropores are observed, as summarized in Table 1. Macropores obtained from n-Si always exhibit a strong growth dependence on crystallographic orientation. On p-Si, this dependency is lower (Lehmann and Rönnebeck 1999), and in aqueous conditions at low enough current density and/or high enough HF concentration, the growth turned to be determined by the direction of the current lines in the space-charge region (Media et al. 2011).

Macropore Formation

Table 2 summarizes the main characteristics of the electrochemically grown macropores on Si, as a function of the formation conditions.

Figure 1 illustrates the variety of pores obtained for p-Si under different conditions.

Table 1 Macropores classes and their main characteristics

Class of macropores	Macropore morphology	Macropore orientation	Remarks	References
Current-line-driven pores	Rounded bottoms	Normal to the surface	Filled with microporous silicon	p-Si, aqu (Wehrspohn et al. 1998)
Crystallography-driven pores	(111) Facets at their bottoms and (110) oriented walls	(100) Preferred growth direction	Empty	n-Si, aqu, bsi: (Lehmann and Föll 1990)
				n-Si, aqu, fsi: (Lévy-Clément et al. 1994)
				p-Si, org: (Propst and Kohl 1994; Ponomarev and Lévy-Clément 1998; Christophersen et al. 2000a)
				p-Si, aqu: (Lehmann and Rönnebeck 1999)

Table 2 General conditions for macropore formation

Formation conditions	Specificity of obtained macropores	References
n-Si (aqu)/bsi	Grow exclusively in <100> direction, dependence of the pore morphology on the sample orientation	Lehmann (1993, 1995), Rönnebeck et al. (1999), Kleimann et al. (2000), and Laffite et al. (2011)
	SCR limits distances; max. depth > 600 µm achieved obtained for $J < J_{PSL}$; arrays with pore diameters 100 µm–250 nm can be obtained	
n-Si (aqu)/fsi	Well-developed macropores oriented <100>	Lévy-Clément et al. (1994) and Outemzabet et al. (2005)
	Not much investigated	
n-Si (org)/bsi	Prone to pore branching and strange morphologies, but regular macropores arrays can be obtained	Christophersen et al. (2000a, b, 2001) and Izuo et al. (2002)
	Not much investigated	
p-Si (aqu)	Obtained at current densities $<J_{PSL}$ and for low-to-medium HF concentration. Easy to make; arrays of high aspect ratio can be obtained	Lehmann and Rönnebeck (1999), Chao et al. (2000), Chazalviel et al. (2002), and Urata et al. (2012)
p-Si (org)	Large macropore observed; decisive parameters are electrolyte resistivity, oxidizing power, and "passivation power"	Ponomarev and Lévy-Clément (2000), Christophersen et al. (2001), and Lust and Lévy-Clément (2002)
n^+-Si (aqu + oxidant)	Small diameter (60–100 nm), high-aspect-ratio macropores	Christophersen et al. (2000c) and Ge et al. (2010)

"Passivation power" denotes the degree to which a given electrolyte can remove interface states in the bandgap of Si by covering a freshly etched surface with hydrogen

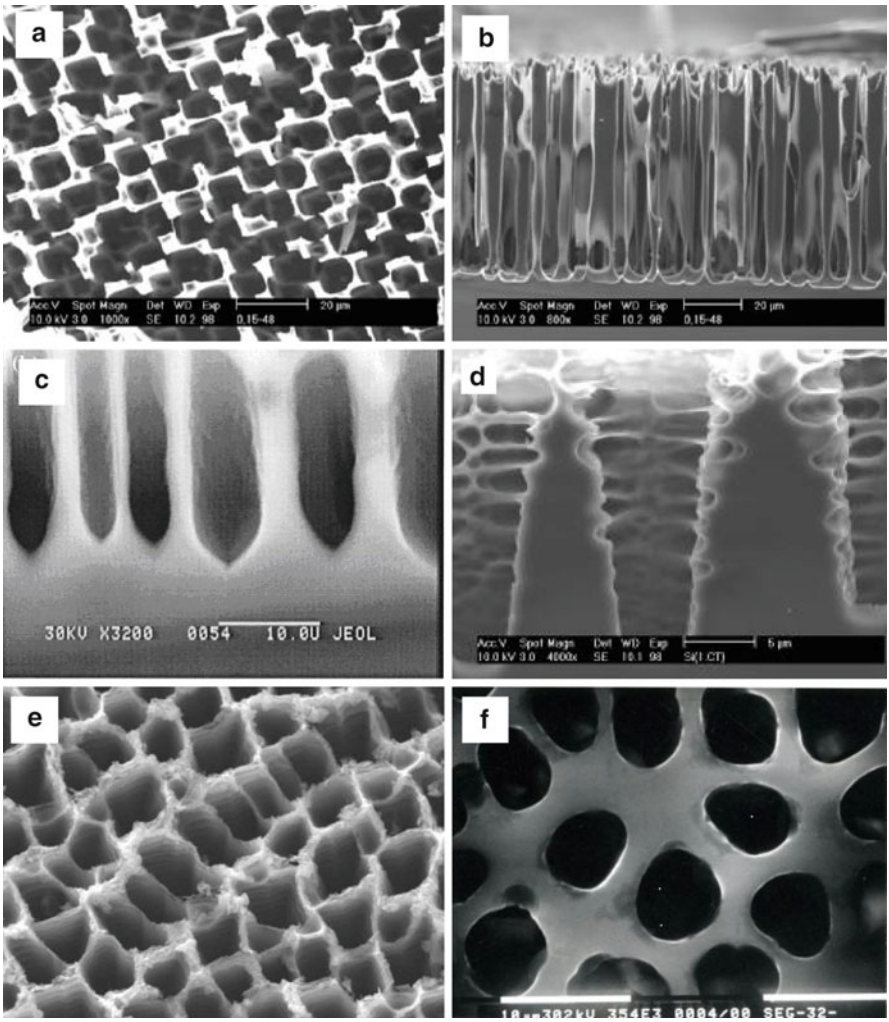

Fig. 1 Morphologies for (100) p-Si in 0.05 M HF, 0.05 M NH4F, and 0.9 M NH4Cl, pH = 3, V = 0.15 V for 48 h: (**a**) Plan view and (**b**) cross section (After Slimani et al. 2009). (**c**) Macropores on p-Si (aqu), view after cleavage, for samples prepared from p-Si (400 Ω cm, (100)-oriented), 100 mA/cm^2, 6 min, 15% ethanolic HF (After Chazalviel et al. 2002). Macropores on (100) n-Si etched in ethanolic hydrofluoric solution with *frontside* illumination and with an anodization current J = 20 mA/cm^2 for t = 45 min. (**d**) Cross-section and (**e**) plan view (After Outemzabet et al. 2005). (**f**) Macropore on p-Si (org) prepared from p-Si (100 Ω cm, 20 mA/cm^2, 40 min, HF/ethylene glycol 50/50 by vol)

Table 3 Major theoretical contributions to macropore formation analysis

Pore formation models	Basis of model	General review
Hole focusing at pore tips	Hole transport across space charge	Lehmann and Föll (1990), Lehmann (1993), and Lehmann and Rönnebeck (1999)
Surface chemical reactions	Pore initiation through limited diffusion of reaction intermediates	Kooij and Vanmaekelbergh (1997) and Vyatkin et al. (2002)
Linear stability analysis	Quantitative assessment of the effect of transport across space charge and reaction kinetics on interface stability	Kang and Jorné (1993, 1997), Valance (1997), Wehrspohn et al. (1999), and Chazalviel et al. (2000, 2002)
The Current Burst Model (CBM)	Spatial and temporal inhomogeneity of current, hydrogen surface passivation	Carstensen et al. (2000) and Föll et al. (2002)

Macropore Formation Models

Porous silicon formation models have been reviewed (Smith and Collins 1992; Allongue 1997; Zhang 2001). A conceptual analysis has been attempted (Zhang 2004). Major theoretical contributions applying to macropore formation are listed in Table 3.

Principal Application of Macropores

Macropore arrays found applications in various fields, some of which are listed in Table 4.

Design of Regular Macropore Arrays

The fabrication of regular macropore arrays requires prestructuring of the Si substrate using lithography and alkaline etching (Chao et al. 2000; van den Meerakker et al. 2000; Starkov 2003). The pitch of the prestructured hole array has to match the average spacing of random macropore arrays grown on the same substrate under similar electrochemical conditions. The width of the walls of the porous structure (which depends on the pitch structure and the pore lateral size) is mostly determined by the width of the space-charge layer (i.e., mostly dependent on substrate doping level) and the pore diameter by the etching conditions. Figures 2 and 3 give some design rules in the case of p-Si. In the case of n-Si, the pore diameter is mostly determined by the current density, i.e., the illumination level, according to Lehmann's model (Lehmann 1993). However, diffusion effects in the liquid phase,

Table 4 Main application domains of macropore arrays

Specific design	Applications area	References
Densely spaced regular macropore arrays	"Brownian motor" or pumps	Schilling et al. (2000a)
Macropores with a sawtooth-like cross section	Membrane (pump of particles)	Kettner et al. (2000) and Schilling et al. (2000b)
Macropores filled with lead, scintillating guide	X-ray imaging	Lehmann and Rönnebeck (2001) and Kleimann et al. (2000)
Macropores coated with (immobilized) biomolecules	Detection of specific biomolecules, DNA, etc.	Bengtsson et al. (2000) and Yoo et al. (2013)
Macropores coated with a catalyst	Chemical reactor	Lehmann et al. (1999)
Macropores coated with high-quality dielectrics	Capacitors	Lehmann et al. (1996)
Macropores on multicrystalline Si	Solar cell – antireflection layer	Föll et al. (1983), Lipiński et al. (2003), and Ao et al. (2012)
Macropores filled with a succession of different metals	Metallic barcodes	Nicewarner-Pena et al. (2001)
Optimized macropore lattices	Photonic bandgap (PBG) materials for optics and sensing	Grüning et al. (1996), Birner et al. (2000), Müller et al. (2000), and Wehrspohn et al. (2013)
Matrix-embedded Si nanowires or particles made from macroporous Si	Lithium-ion batteries	Föll (2010) and Thakur et al. (2012)
Sacrificial or template macroporous Si layer	Micromachining or microelectronics	Steiner and Lang (1995) and Defforge et al. (2013)

as theoretically modeled (Barillaro and Pieri 2005), must be taken into account in order to keep the fluoride concentration stationary at the pore tips. Figure 4 gives the typical pore-density range accessible on n-Si under usual backside illumination conditions or p-Si in the dark.

Conclusions

Since the first report of Theunissen (1972) and the pioneering work of Lehmann in the 1990s, many efforts have been devoted to macropore fabrication by electrochemical etching. Impressive macropore arrays have been achieved, with high aspect ratios and smooth or patterned vertical walls. Examples are shown in Fig. 5. Alternative techniques have been proposed such as galvanic etching (Xia et al. 2000), stain etching (Mills et al. 2005), and metal-assisted (electro)chemical etching (Li et al. 2013). These techniques are separately reviewed in this handbook (see chapters ▶ "Porous Silicon Formation by Galvanic Etching," ▶ "Porous Silicon Formation by Stain Etching," and ▶ "Porous Silicon Formation by Metal Nanoparticle-Assisted Etching").

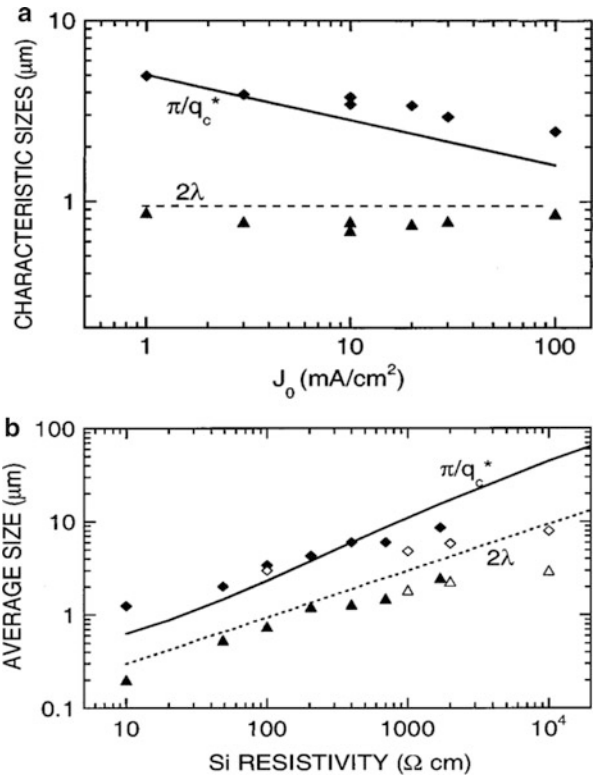

Fig. 2 Comparison of characteristic macropore sizes on p-Si in the current-line-driven regime, when changing current density for a substrate resistivity of 100 Ω cm (**a**) and silicon doping for an applied current density of 10 mA/cm^2 (**b**) (After Chazalviel et al. 2002). Triangles refer to the wall width and diamonds to the pore diameter; the closed (open) symbols refer to the data obtained in 35% (25%) ethanolic HF. The *solid lines* refer to the theoretical prediction (Chazalviel et al. 2002) for the pore diameter, and the *dotted line* is two times the space-charge width λ

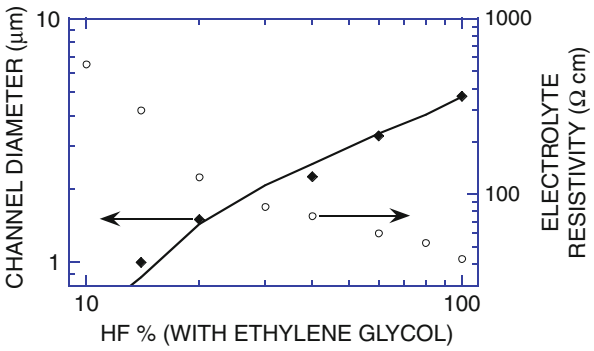

Fig. 3 Effect of changing electrolyte resistivity on average macropore diameter on p-Si 1,500 Ω cm, for $J_0 =$ 10 mA/cm^2 in an electrolyte made of 50% aqueous HF mixed with ethylene glycol in variable proportions (After Chazalviel et al. 2002)

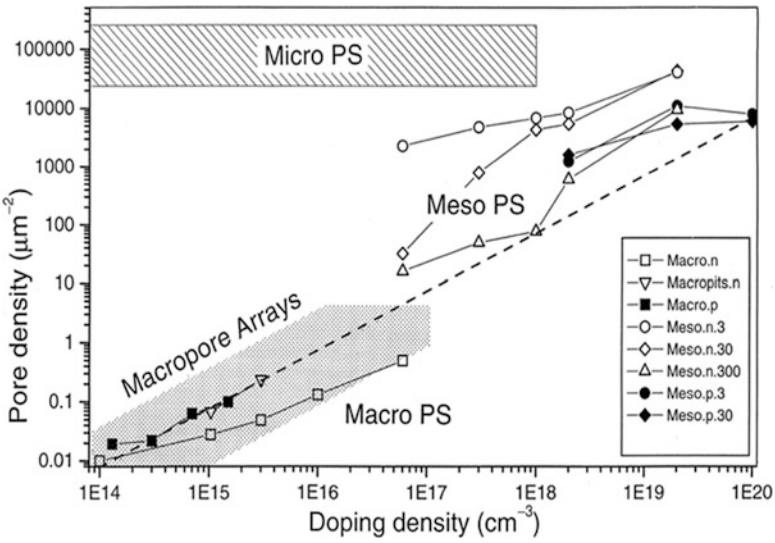

Fig. 4 Pore density versus silicon electrode doping density for porous silicon layers of different geometries. Notice that macropores are essentially obtained on low to moderately doped substrates. The *dashed line* shows the pore density of a triangular pore pattern with a pore pitch equal to two times the SCR width for a 3 V applied bias. Note that only macropores on n-type substrates may show a pore spacing significantly exceeding this limit. The regime of stable macropore array formation on n-Si is indicated by a dot pattern. Doping type and etching current density (in mA/cm^2) are indicated in the legend (After Lehmann 1993)

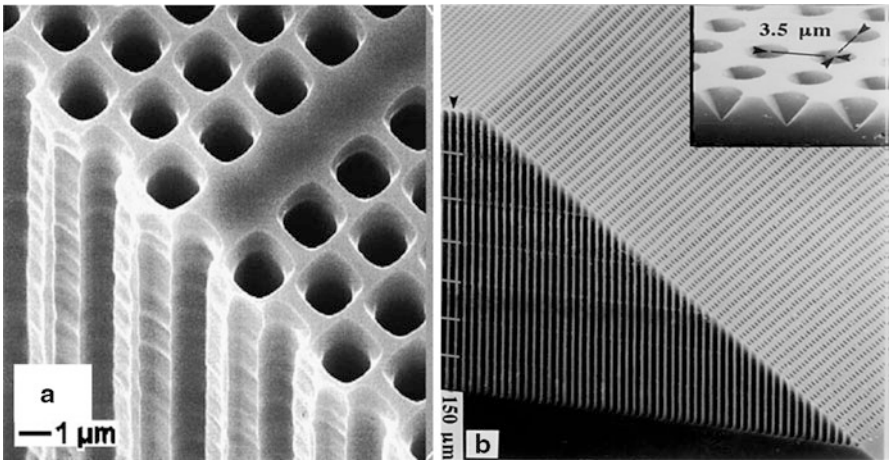

Fig. 5 Examples of regular and ordered macropore arrays. (**a**) Two-dimensional macropore array with an intentional line defect (From Grüning et al. 1996); (**b**) array of pores grown on n-Si (10^{15} cm^{-3}); the pore initiation pattern shown in the inset has been produced by photolithography and alkaline etching (From Lehmann et al. 2000)

References

Allongue P (1997) Porous silicon formation mechanisms. In: Canham L (ed) Properties of porous silicon, EMIS Data Review No 18, Chapter 1.1, INSPEC-IEE, pp 3–11

Ao X, Tong X, Kim DS, Zhang L, Knez M, Müller F, He S, Schmidt V (2012) Black silicon with controllable macropore array for enhanced photoelectrochemical performance. Appl Phys Lett 101:111901

Barillaro G, Pieri F (2005) A self-consistent theoretical model for macropore growth in n-type silicon. J Appl Phys 97:116105

Bengtsson M, Ekström S, Drott J, Collins A, Csöregi E, Marko-Varga G, Laurell T (2000) Applications of microstructured porous silicon as a biocatalytic surface. Phys Stat Sol 182:495–504

Birner A, Li A-P, Müller F, Gösele U, Kramper P, Sandoghdar V, Mlynek J, Busch K, Lehmann V (2000) Transmission of a microcavity structure in a two-dimensional photonic crystal based on macroporous silicon. Mat Sci Semicon Proc 3:487–491

Carstensen J, Christophersen M, Föll H (2000) Pore formation mechanisms for the Si-HF system. Mat Sci Eng B 69/70:23–28

Chao KJ, Kao SC, Yang CM, Hseu MS, Tsai TG (2000) Formation of high aspect ratio macropore array on p-type silicon. Electrochem Solid St Lett 3:489–492

Chazalviel J-N, Ozanam F (2005) Macropores in p-type silicon. In: Wehrspohn RB (ed) Ordered porous nanostructures and applications, Chapter 2. Springer, New York, pp 15–35

Chazalviel J-N, Wehrspohn RB, Ozanam F (2000) Electrochemical preparation of porous semiconductors: from phenomenology to understanding. Mat Sci Eng B 69/70:1–10

Chazalviel J-N, Ozanam F, Gabouze N, Fellah S, Wehrspohn RB (2002) Quantitative analysis of the morphology of macropores on low-doped p-Si minimum resistivity. J Electrochem Soc 149: C511–C520

Christophersen M, Carstensen J, Föll H (2000a) Crystal orientation dependence of macropore formation in p-type silicon using organic electrolytes. Phys Status Solidi A 182:103–107

Christophersen M, Carstensen J, Feuerhake A, Föll H (2000b) Crystal orientation and electrolyte dependence for macropore nucleation and stable growth on p-type Si. Mat Sci Eng B 69–70:194–198

Christophersen M, Carstensen J, Föll H (2000c) Macropore formation on highly doped n-type silicon. Phys Status Solidi A 182:45–50

Christophersen M, Carstensen J, Rönnebeck S, Jäger C, Jäger W, Föll H (2001) Crystal orientation dependence and anisotropic properties of macropore formation of p- and n-type silicon. J Electrochem Soc 148:E267–E275

Defforge T, Coudron L, Ménard O, Grimal V, Gautier G, Tran-Van F (2013) Copper electrodeposition into macroporous silicon arrays for through silicon via applications. Microelectron Eng 106:160–163

Föll H, Hartz H, Ossei-Wusu E, Carstensen J, Riemenschneider O (2010) Si nanowire arrays as anodes in Li ion batteries. Phys Status Solidi RRL 4:4–6

Föll H, Christophersen M, Carstensen J, Hasse G (2002) Formation and application of porous silicon. Mat Sci Eng R 280:1–49

Föll H, Grabmaier J, Lehmann V (1983) Process for producing crystalline silicon bodies having a structure which increases the surface area, and use of said bodies as substrates for solar cells and catalysts. German Patent DE 3324232

Ge DH, Jiao JW, Zhang S, Wang YL (2010) Fast speed nano-sized macropore formation on highly-doped n-type silicon via strong oxidizer. Electrochem Commun 12:603–606

Grüning U, Lehmann V, Ottow S, Busch K (1996) Macroporous silicon with a complete two-dimensional photonic band gap centered at 5 μm. Appl Phys Lett 68:747–749

Izuo S, Ohji H, French PJ, Tsutsumi K (2002) A novel electrochemical etching technique for n-type silicon. Sens Actuat A 97–98:720–724

Kang Y, Jorné J (1993) Porous silicon formation: morphological stability analysis. J Electrochem Soc 140(2258–2265)
Kang Y, Jorné J (1997) Dissolution mechanism for p-Si during porous silicon formation. J Electrochem Soc 144:3104–3111
Kettner C, Reimann P, Hänggi P, Muller F (2000) Drift ratchet. Phys Rev E 61:312–323
Kleimann P, Linnros J, Petersson S (2000) Formation of wide and deep pores in silicon by electrochemical etching. Mater Sci Eng B 69–70:29–33
Kooij S, Vanmaekelbergh D (1997) Catalysis and pore initiation in the anodic dissolution of silicon in HF. J Electrochem Soc 144:1296–1301
Laffite G, Roumanie M, Gourgon C, Perret C, Boussey J, Kleimann P (2011) Formation of submicrometer pore arrays by electrochemical etching of silicon and nanoimprint lithography. J Electrochem Soc 158:D10–D14
Lehmann V (1993) The physics of macropore formation in low doped n-type silicon. J Electrochem Soc 140:2836–2843
Lehmann V (1995) The physics of macroporous silicon formation. Thin Solid Films 255:1–4
Lehmann V (2002) Chapter 9, Macroporous silicon. In: Electrochemistry of silicon. Wiley-VCH, Weinheim
Lehmann V (2005) Electrochemical pore array fabrication on n-type silicon electrodes. In: Wehrspohn RB (ed) Ordered porous nanostructures and applications, Chapter 1. Springer, New York, pp 3–13
Lehmann V, Föll H (1990) Formation mechanism and properties of electrochemically etched trenches in n-type silicon. J Electrochem Soc 137:653–659
Lehmann V, Rönnebeck S (1999) The physics of macropore formation in Low-doped p-type silicon. J Electrochem Soc 146:2968–2975
Lehmann V, Rönnebeck S (2001) MEMS techniques applied to the fabrication of anti-scatter grids for X-ray imaging. Sensor Actuator A 95:202–207
Lehmann V, Hönlein W, Reisinger H, Spitzer A, Wendt H, Willer J (1996) A novel capacitor technology based on porous silicon. Thin Solid Films 276:138–142
Lehmann V, Ottow S, Stengl R, Reisinger H, Wendt H (1999) Reactor system and corresponding production method. European Patent WO 9961147
Lehmann V, Stengl R, Luigart A (2000) On the morphology and the electrochemical formation mechanism of mesoporous silicon. Mat Sci Eng B 69–70:11–22
Lévy-Clément C, Lagoubi A, Tomkiewicz M (1994) Morphology of porous n-type silicon obtained photoelectrochemical etching: correlation with material and etching parameters. J Electrochem Soc 141:958–967
Li Z, Zhao L, Diao H, Li H, Zhou C, Wang W (2013) Preparation of large-aperture macroporous silicon with controllable pore tip angle on low-resistivity p-type c-Si substrate by metal-catalyzed electrochemical etching. ECS J Solid State Sci Technol 2:Q65–Q68
Lipiński M, Bastide S, Panek P, Lévy-Clément C (2003) Porous silicon antireflection coating by electrochemical and chemical etching for silicon solar cell manufacturing. Phys Status Solidi (a) 197:512–517
Lust S, Lévy-Clément C (2002) Chemical limitations of macropore formation on medium-doped p-type silicon. J Electrochem Soc 149:C338–C344
Media EM, Chazalviel J-N, Ozanam F, Outemzabet R (2011) Current-line driven macropores: which current? Phys Status Solidi (c) 8:1727–1730
Mills D, Nahidi M, Kolasinski KW (2005) Stain etching of silicon pillars and macropores. Phys Status Solidi (a) 202:1422–1426
Müller F, Birner A, Gösele U, Lehmann V, Ottow S, Föll H (2000) Structuring of macroporous silicon for applications as photonic crystals. J Porous Mat 7:201–204
Nicewarner-Pena SR, Freeman RG, Reiss BD, He L, Pena DJ, Walton ID, Cromer R, Keating CD, Natan MJ (2001) Submicrometer metallic barcodes. Science 294:137–141

Outemzabet R, Gabouze N, Kesri N, Cheraga H (2005) Random macropore formation in n-type silicon under front side illumination: correlation with anisotropic etching. Phys Status Solidi (c) 2:3394–3398

Ponomarev EA, Lévy-Clément C (1998) Macropore formation on p-type Si in fluoride containing organic electrolytes. Electrochem Solid St Lett 1:42–45

Ponomarev EA, Lévy-Clément C (2000) Macropore formation on p-type silicon. J Porous Mat 7:51–56

Propst EK, Kohl PA (1994) The electrochemical oxidation of silicon and formation of porous silicon in acetonitrile. J Electrochem Soc 141:1006–1013

Rönnebeck S, Carstensen J, Ottow S, Föll H (1999) Crystal orientation dependence of macropore growth in n-type silicon. Electrochem Solid St Lett 2:126–128

Schilling J, Müller F, Birner A, Gösele U, Kettler C, Hänggi P (2000a) Membranes for micropumps from macroporous silicon. Phys Status Solidi (a) 182:585–590

Schilling J, Müller F, Matthias S, Wehrspohn RB, Gösele U (2000b) Three-dimensional photonic crystals based on macroporous silicon with modulated pore diameter. Appl Phys Lett 78:1180–1182

Slimani A, Iratni A, Chazalviel J-N, Gabouze N, Ozanam F (2009) Experimental study of macropore formation in p-type silicon in a fluoride solution and the transition between macropore formation and electropolishing. Electrochim Acta 54:3139–3144

Smith RL, Collins SD (1992) Porous silicon formation mechanisms. J Appl Phys 71:R1–R22

Starkov VV (2003) Ordered macropore formation in silicon. Phys Status Solidi (a) 197:22–26

Steiner P, Lang W (1995) Micromachining applications of porous silicon. Thin Solid Films 255:52–58

Thakur M, Pernites RB, Nitta N, Isaacson M, Sinsabaugh SL, Wong MS, Biswal SL (2012) Freestanding macroporous silicon and pyrolyzed polyacrylonitrile as a composite anode for lithium ion batteries. Chem Mat 24:2998–3003

Theunissen MJJ (1972) Etch channel formation during anodic dissolution of n-type silicon in aqueous hydrofluoric acid. J Electrochem Soc 119:351–360

Urata T, Fukami K, Sakka T, Ogata YH (2012) Pore formation in p-type silicon in solutions containing different types of alcohol. Nanoscale Res Lett 7:329

Valance A (1997) Theoretical model for early stages of porous silicon formation from n- and p-type silicon substrates. Phys Rev B 55:9706–9715

van den Meerakker JEAM, Elfrink RJG, Roozeboom F, Verhoeven JFCM (2000) Etching of deep macropores in 6 in Si wafers. J Electrochem Soc 147:2757–2761

Vyatkin A, Starkov V, Tzeitlin V, Presting H, Konle J, König U (2002) Random and ordered macropore formation in p-type silicon. J Electrochem Soc 149:G70–G76

Wehrspohn RB, Chazalviel J-N, Ozanam F (1998) Macropore formation in highly resistive p-type crystalline silicon. J Electrochem Soc 145:2958–2961

Wehrspohn RB, Ozanam F, Chazalviel J-N (1999) Nano- and macropore formation in p-type silicon. J Electrochem Soc 146:3309–3314

Wehrspohn RB, Schweizer SL, Gesemann B, Pergande D, Geppert TM, Moretton S (2013) Macroporous silicon and its application in sensing. A Lambrecht C R Chim 16:51–58

Xia XH, Ashruf CMA, Franck PJ, Kelly JJ (2000) Galvanic cell formation in silicon/metal contacts: the effect on silicon surface morphology. Chem Mat 12:1671–1678

Yoo L, Ahn K-Y, Ahn J-Y, Laurell T, Lee YM, Yoo PJ, Lee J (2013) A simple one-step assay platform based on fluorescence quenching of macroporous silicon. Biosens Bioelectron 41:477–483

Zhang XG (2001) Chapter 8, Porous silicon. In: Electrochemistry of silicon and its oxide. Springer, New York

Zhang XG (2004) Morphology and formation mechanisms of porous silicon. J Electrochem Soc 151:C69–C80